Available online at www.sciencedirect.com

ScienceDirect

Solar Energy 116 (2015) 303–313

SOLAR ENERGY

www.elsevier.com/locate/solener

Large scale PV systems under non-uniform and fault conditions

J.P. Vargas *, B. Goss, R. Gottschalg

Centre for Renewable Energy Systems Technology (CREST), School of Electronic, Electrical and Systems Engineering, Loughborough University, LE11 3TU England, United Kingdom

Received 12 January 2015; accepted 23 March 2015
Available online 29 April 2015

Communicated by: Associate Editor Bibek Bandyopadhyay

Abstract

Current codes of practice for PV systems lack detailed guidance regarding circuit mismatch, over or reverse current protection and unbalanced operational conditions in large PV systems. Experimental work in this field is expensive and limited by hardware and environmental resources. The available commercial simulation tools do not rigorously model the complex behaviour of PV systems operating under non-uniform conditions. In this paper a detailed cell-by-cell model of large scale PV systems is developed. The parameter set used for simulations is based on real PV modules power tolerance data and the variance in its principal parameters, thus representing a realistic power frequency distribution. The model is used to estimate and analyse losses due to circuit mismatch, analyse the causes of reverse current in the system's strings and its consequences in the system performance and to estimate energy losses due to string's fuses failures.

Keywords: Detailed model; Fuses failures; Mismatch losses; Non-uniform conditions; System performance; Reverse current

1. Introduction

Pressures on PV system developers to deliver improved the economic returns is motivating research in systems optimization to minimize losses, and deliver improvements in systems reliability to minimize components failures.

One of the inherent losses of PV systems is the mismatch due to electrical interconnection. The manufacturing tolerances for PV modules result in a variation in their physical parameters. When a PV system is formed from modules with variation in their parameters, losses appear due to circuit mismatch in the electrical connections. This is because each PV module has a different maximum power point, so each module has to operate at non-ideal current and voltage to conform to Kirchhoff's Law. When connected together in series, all modules will operate at the same current. In parallel connections, all strings (of modules) will operate at the same voltage. Therefore each module operates away from its maximum power point and the system power is not the sum of the power of the modules.

The operation at the same operating voltage may cause reverse currents that are another source of losses. This may be an issue particularly in large PV systems with large number of strings. The system voltage may be higher than a particular string voltage, thus causing a reverse current in this string. The reason for the imbalance voltage can be unbalanced operating conditions (shadowed panels) or failures (short-circuits) in a string. It is not clear what is the magnitude of this reverse current and if fuses are appropriate to prevent energy loss and damage to components.

Estimating the losses and consequences of unbalanced operational conditions with experimental work is expensive and limited by hardware resources and environmental variables. Computer simulation offers control over all the variables in a PV system, therefore more defined results can be

* Corresponding author. Tel.: +56 224604269.
E-mail address: j.p.vargas-abalos-12@alumni.lboro.ac.uk (J.P. Vargas).

http://dx.doi.org/10.1016/j.solener.2015.03.041
0038-092X/

obtained. The available commercial simulation tools, do not rigorously model the complex behaviour of PV systems operating under non-uniform conditions, therefore a detailed model of large PV systems need to be developed.

The aim of this paper is to estimate and analyse losses in PV systems due to variations in the parameters of the modules and to analyse the magnitude of reverse currents in the strings as well as the consequences on system performance. The objectives of the paper are to:

- Develop a detailed model of large scale PV systems.
- Generate different distributions of PV module parameters, according to available statistic data.
- Estimate and analyse losses due to circuit mismatch.
- Analyse the causes and consequences of reverse current in the system's strings.
- Estimate losses due to string fuse failures using its mean time to failure (MTTF).

2. Methodology

2.1. System model

The single diode model based simulation introduced by Bishop (1988) develops at a cell level (cell by cell) methodology. This method is adapted here by using a Newton Raphson solver as suggested e.g. by Quaschning et al. (Quaschning and Hanitsch, 1996). It was decided to not incorporate the two diode model as this would just add complexity without any gain in accuracy.

$$f(V,I) = I_{SC} - I_0 \cdot \left(\exp\left(\frac{q(V + I \cdot R_S)}{m \cdot k \cdot T}\right) - 1\right) - \frac{V + I \cdot R_S}{R_{SH}} - I \equiv 0 \quad (1)$$

Each PV module is composed of a series of substrings, as described in Johansson et al. (2004), Mohapatra (2011) and Goss et al. (2014). A substring is a series of cells in parallel with a bypass diode; therefore the current passing through a substring is the sum of the current passing through the series of cells and the current passing through the bypass diode. The bypass diode only can conduct current if the voltage of the series of cells is lower than the critical voltage of the bypass diode obtained from Eq. (2). The voltage of the bypass diode must be equal to the voltage of the series of cells (sum of the voltages of each cell for a specific current). When the diode is conducting current, the voltage in the diode (and the voltage in the series of cells) can be obtained from Eq. (3).

$$V_{Crit} = -\frac{m_D \cdot k \cdot T}{q} \cdot \ln\left(\frac{m_D \cdot k \cdot T}{q \cdot \sqrt{2} \cdot I_{0_D}}\right) \quad (2)$$

$$f(V,I) = I_{0_D} \cdot \left(\exp\left(\frac{-q(V + I \cdot R_{S_D})}{m_D \cdot k \cdot T}\right) - 1\right) \equiv 0 \quad (3)$$

Each string is composed by a series of PV modules (that are a series of substrings). Parallel connections were added to the Mohapatra model (Mohapatra, 2011), forming a PV array composed by strings connected in parallel. To solve the I–V curve of the array, first the I–V curve of each string is solved summing the voltage of each substring for a specific string current. The I–V curve of the array is then solved summing the strings currents for a specific array voltage.

2.2. PV modules parameters distributions

In order to evaluate the circuit mismatch of the system, parameter variation was introduced into the cell model parameters to simulate realistic module power tolerances. These were matched on flash test data available to the authors from different projects. The cell parameters varied were the series resistance R_S, the shunt resistance R_{SH}, the short circuit current I_{SC} and the dark-current I_0, as described by Herrmann (2005). The cell parameters were generated using two types of distribution, normal distribution and realistic distribution obtained from manufacturer's flash tests data. Two commercial modules were considered, a standard silicon module and a high efficiency silicon module. Data of 210 flash tests of each type was used for the realistic distributions.

For the normal distributions, the parameters were generated using Eq. (4), where x is the parameter, σ is the standard deviation, r is a Gaussian random number and $\bar{x}$ is the mean value of the parameter. The mean value and the standard deviation were obtained from the datasheets of the modules.

$$x = \sigma \cdot r + \bar{x} \quad (4)$$

For the realistic distribution, a regression method was used to fit the distribution the best possible with the real distribution obtained from the data of the flash tests of the modules and considering the sorting in power categories done by the manufacturers.

2.3. Power and energy simulations

Instead of the mismatch degradation factor used by MacAlpine et al. (2012), simulations were performed to evaluate the mismatch losses, considering different systems sizes (kWp). Power simulations were considered to evaluate the static losses, using Herrmann (2005), and also dynamic energy simulations were performed taking into account the action of a central inverter to set the optimum operational point of the system (maximum power point MPP), in contrast with Gomez et al. (2014) that used a simplified method.

The cell model has static and dynamic parameters. Static parameters are R_S, R_{SH} and m, which remain constant under all physical conditions. Dynamic parameters are I_{SC}, E_g, I_0 and V_{OC}, which present a dependence on temperature T and irradiance G as shown in Eqs. (5)–(8).

$$I_{SC}(T,G) = (I_{SC_{STC}} + K_i \cdot (T - T_{STC})) \cdot \frac{G}{G_{STC}} \quad (5)$$

$$E_g(T) = E_g(0) - \frac{\alpha \cdot T^2}{T + \beta} \quad (6)$$

$$I_0(T) = I_{0_{STC}} \cdot \left(\frac{T}{T_{STC}}\right)^3 \cdot \exp\left(\frac{q \cdot E_g}{m \cdot k} \cdot \left(\frac{1}{T_{STC}} - \frac{1}{T}\right)\right) \quad (7)$$

$$V_{OC}(T,G) = \frac{m \cdot k \cdot T}{q} \cdot \ln\left(\frac{I_{SC}}{I_0} + 1\right) \quad (8)$$

For power simulations, STC conditions were considered. For energy simulations, annuals simulations were considered with a time resolution of one hour, namely, the temperature and the irradiance were updated for each hour of the year. The meteorological data of Sutton Bonington[1] obtained from the Met Office Integrated Data Archive System[2] have been used for the energy simulations.

2.4. Strings reverse current analysis

In order to analyse the reverse current that may be present in the strings, the system model was submitted to unbalanced operational conditions that can cause reverse or fault current, as described by Laschinsky et al. (2010) and Goss et al. (2011), considering two scenarios, shading and short-circuits.

For each condition (shading and short-circuit), two PV systems were considered, one using standard silicon modules and the other using high efficiency silicon modules. For each PV system, the system size (installed capacity) was changed, increasing the system current (adding more strings) and/or increasing the system voltage (adding more modules per string), with the aim of identifying the effect in the reverse current of the shaded and short-circuited string when the system size changes.

2.5. Fuses failures and their impact on system performance

In Section 2.4 the effect of reverse current in the strings was analysed including possible fuse failure. The option of fuse failures due to other failures in the system was also included, considering a mean time to failure MTTF. The MTTF was generated using a Weibull distribution described in Eq. (9), where α is the location parameter, λ is the scale parameter, x is a uniformly distributed random number and k is the shape parameter.

$$\text{MTTF} = \alpha + \lambda \cdot (-\ln(x))^{\frac{1}{k}} \quad (9)$$

[1] Sutton Bonington is a village and civil parish lying along the valley of the River Soar in the Borough of Rushcliffe, south west Nottinghamshire, England.

[2] Land surface and marine surface observations data from the Met Office station network and other worldwide stations are stored in the Met Office MIDAS database.

For DC fuses, a failure rate of 1–2 failures per system lifetime increasing with time ($\alpha = 0, \lambda = 1.75 \cdot 10^5$ and $k = 1.5$) was used, as described in Perdue and Gottschalg (2015).

An annual simulation of a 1 MWp system was performed, registering the generation of each string for each hour of the year to identify the failure of a string fuse and therefore the loss of generation. Then simulations were performed for 25 consecutive years, using the same meteorological data and using the string generation data of the 1 MWp system. In each simulation new fuses were included with their respective MTTF. Different inspection periods were performed, where the failed fuses were replaced, generating new fuses with a new MTTF.

3. Results and discussion

3.1. PV modules parameters distributions

Fig. 1 shows the parameter distribution of real and simulated standard silicon modules. The blue line shows the parameters distribution of 210 flash tests of real modules, the red line shows a simulated realistic distribution adjusted from the flash tests data and the black line shows a simulated normal distribution with mean value and standard deviation obtained from the datasheets of the modules. For the simulation of the distributions, 200 modules were simulated for each type of distribution. In the figure, I_{sc} corresponds to the short circuit current, V_{oc} is the open circuit voltage; I_{mp}, V_{mp} and P_{mp} are the current, voltage and power at the maximum power point of the module.

The distribution of the parameters of the real modules (blue line) does not present a normal distribution shape, due to cell sorting into power categories by the manufacturer, resulting in the sharp edge in the high and low power limit of the distribution as shown in Fig. 1. The sorting by power is not a homogeneous process but usually varies in each production order or project contract. Other characteristics of the distribution are that the peak power probability (highest number of modules with the same power bin) of the real modules is not at the central point of the distribution, it is close to the high limit, allowing to keep the power average of the distribution when more lower power modules are added.

A similar result was obtained for the high efficiency modules, but with a very marked highest power probability, demonstrating a strict power selection method (See Fig. A.9 of Appendix A).

Once the distributions were adjusted, 200 simulations of each module type (standard silicon and high efficiency) were performed, using the normal and the real distribution, with the aim of verifying that the parameter variance was in accordance with the datasheet of the modules. Table 1 shows the results of the module simulations. Figs. A.10 and A.11 in Appendix A show the random generation of the standard silicon and high efficiency module parameters.

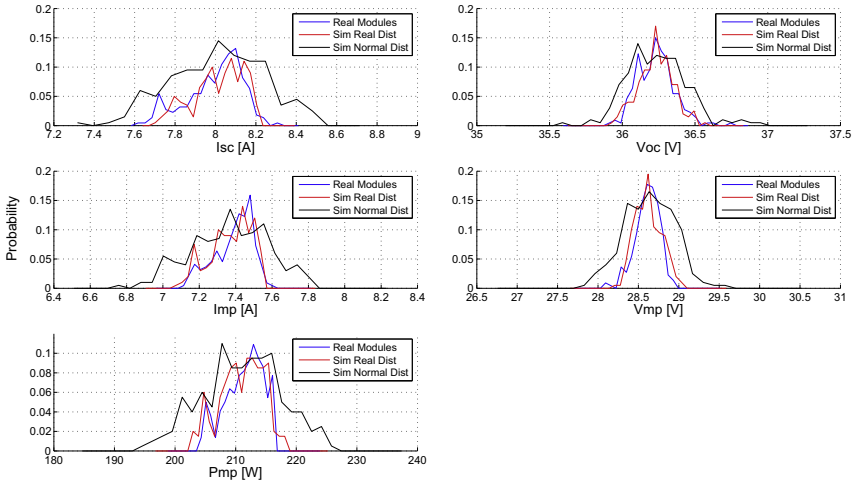

Fig. 1. Standard silicon module parameters distributions.

These are for both distributions (normal and real), and also show the effect of the sorting of power present in the real distribution, resulting in the peak values being closer to the average value than in the normal distribution.

3.2. Power simulations

With the adjusted distributions, 100 PV systems were simulated considering an installed capacity (kW at STC) of 10, 50, 100, 250, 500, 750 and 1000 kWp, using the standard silicon modules. A maximum system voltage of 1000 [VDC] was used in compliance with the voltage limit for IEC-60364 (2005). Each string was formed with 24 modules obtaining a power of 5 kWp per string and an approximate system Voc of 869 [VDC]. Table B.2 in Appendix B, shows the results of the power simulations. Fig. 2 shows the power losses due to the circuit mismatch in a boxplot[3].

Power losses due to circuit mismatch tend to stabilise for systems over 250 kWp, with losses of 0.73% for the normal distribution and with losses of 1.33% for the real distribution. The key finding here is that realistic distributions cause higher power losses than Gaussian distributions, with the order of magnitude of 50% of the bin-width.

3.3. Energy simulations

Annual simulations were conducted with a time resolution of one hour. The target was to perform 100 simulations for each PV system (10, 50, 100, 250, 500, 750 and 1,000 kWp) and for each distribution (Normal and Real). In each simulation a new system was created using the respective distribution to generate the parameters of the modules. Table B.3 in Appendix B, shows the results of the energy simulations. Fig. 3 shows the energy losses due to the circuit mismatch.

As can be seen in Fig. 2 and in Fig. 3, the standard deviation of the losses decreases as the size of the system increases. This is because larger systems have more modules, therefore there is a higher probability that modules with below average power compensate for modules with above average power, thereby decreasing the standard deviation of the whole system.

Energy losses due to circuit mismatch tend to stabilise for systems over 250 kWp, with losses of 1.18% for the normal distribution and losses of 1.73% for the real distribution. This behaviour is similar to the power, but the impact is higher, with the energy loss being closer to 2/3 of the bin-width.

3.4. Strings reverse current analysis

To analyse the reverse current in strings of PV systems under unbalanced conditions, two scenarios were considered: shading and short-circuits, both under STC conditions. Fig. 4 shows a system of 2 strings with 1 string of shaded modules in Fig. 4(a) and with 1 string with modules short-circuited in Fig. 4(b). The blue line is the I–V curve of the whole system and the dashed black lines are the I–V curves of each string (the shaded/short-circuited and the normal). The magenta line is the power of the system and the red line is the reverse current in the shaded or short-circuited string. The asterisk is the reverse current at the voltage of the maximum power point of the system (MPP) and the triangle is the reverse current at the open circuit voltage (Voc) of the system. For simplicity, in the following graphs only the curve corresponding to the reverse current will be showed. When the system conditions change suddenly, like in a short-circuit, the inverter takes time to find the new maximum power point of the system, therefore there is a transient fault current, that is the current between the

[3] Boxplot is a convenient way of graphically depicting groups of numerical data through their quartiles with the box and their extreme values with the tip lines.

Table 1
Modules parameters distributions.

Parameters distributions									
	Standard silicon modules Datasheet information					High efficiency modules Datasheet information			
	V_{OC} [V]	I_{SC} [A]	P_{mp} [W]	V_{mp} [V]	I_{mp} [A]	V_{OC} [V]	I_{SC} [A]	P_{mp} [W]	V_{mp} [V]	I_{mp} [A]
	36	7.8	210 ± 3%	29.5	7.2	48.5	5.87	225 ± 3%	41	5.49
	Simulations with normal distribution					Simulations with normal distribution				
	V_{OC} [V]	I_{SC} [A]	P_{mp} [W]	V_{mp} [V]	I_{mp} [A]	V_{OC} [V]	I_{SC} [A]	P_{mp} [W]	V_{mp} [V]	I_{mp} [A]
Average	36.20	7.99	210.08	28.59	7.35	49.01	5.89	225.17	41.08	5.48
Std. dev. [%]	0.66	3.04	3.09	1.07	3.04	0.95	2.49	3.15	1.48	2.53
Max.	37.02	8.68	229.88	29.48	8.00	51.05	6.31	242.17	43.16	5.87
Min.	35.66	7.37	193.80	27.76	6.78	47.93	5.57	207.94	39.29	5.18
	Simulations with real distribution					Simulations with real distribution				
	V_{OC} [V]	I_{SC} [A]	P_{mp} [W]	V_{mp} [V]	I_{mp} [A]	V_{OC} [V]	I_{SC} [A]	P_{mp} [W]	V_{mp} [V]	I_{mp} [A]
Average	36.23	8.00	210.41	28.61	7.35	48.99	5.94	226.40	40.97	5.53
Std. dev. [%]	0.72	2.81	3.02	1.18	2.81	0.89	2.65	3.03	1.30	2.69
Max.	37.34	8.34	225.25	29.67	7.68	50.32	6.18	238.91	42.64	5.74
Min.	35.45	7.39	194.54	27.82	6.78	47.92	5.03	191.68	39.19	4.67

diamond and the asterisk in Fig. 4(b) and its duration time depends of the response of the MPP tracking algorithm during the fault.

For the reverse current analysis, for both scenarios (shading and short circuits) were tested on two systems, one system using standard silicon modules and another system using high efficiency modules. For the standard silicon system, a power of 50 kWp was considered, with a system composed by 10 strings of 24 modules per string and an approximate system Voc of 864 [VDC]. For the high efficiency system, a power of 40 kWp was considered, with a system composed by 10 strings of 18 modules per string and an approximate system Voc of 873 [VDC]. Fig. 5(a) shows the reverse current present in one string when different numbers of modules in the string are shaded by 90%. Fig. 5(b) shows the reverse current present in one string when different numbers of modules of the string are short-circuited. For both figures the continuous lines are for the standard silicon system and the dashed lines are for the high efficiency system.

As can be seen in Fig. 5(a), when the inverter is working optimally (tracking the maximum power point of the system), there is no reverse current in the shaded string at the voltage of the maximum power point of the system. If the inverter switches off for any reason, the voltage of the system will be Voc and the reverse current present in a completely shaded string (a 90% irradiance reduction affecting all modules), will not exceed the short circuit current of the modules. Grid connected PV inverters tested to IEC-62109 (2010) must include protection which disconnects the inverter from the utility network in the event of an array earth fault or the AC voltage or frequency going outside the allowable range. The latter protection type may occur if there is a fault in the AC network for example a high resistance joint causing excessive voltage rise.

As shown in Fig. 5(b), when the inverter is operating, it is necessary for 10 of 24 modules to be short-circuited to cause a reverse current fault of more than twice the Isc for the standard silicon system and 6 of 18 modules for the high efficiency system. This reverse fault current (◇ in the figure) will start to decrease after the fault as the inverter is tracking the new MPP of the system (∗ for standard silicon system and x for high efficiency system). When the inverter is off (the voltage of the system is Voc), it is necessary to short-circuit 6 of 24 modules to have a reverse current around twice the Isc for the standard silicon system and 3 of 18 modules for the high efficiency.

A reverse current of three times the short circuit current would limit the temperature increase due to the reverse current within tolerable limits, keeping cell operating temperatures below 100 °C (Calais et al., 2008). With a cell operating temperature of 100 °C, some parts of the encapsulation of the module will be damaged, therefore for this paper a reverse current over two times Isc will be considered dangerous. The IEC Standard for PV Fuses (IEC-60269, 2010) specifies a non fusing current $I_{nf} = 1.13 \cdot I_n$

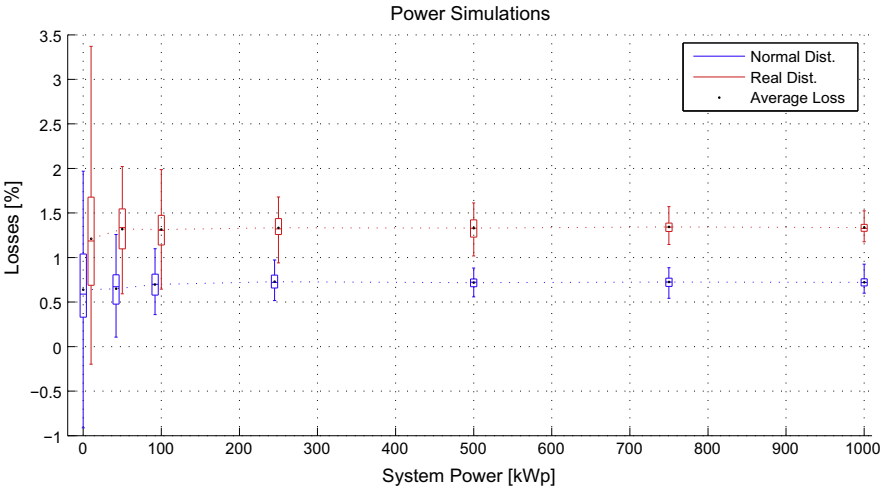

Fig. 2. Power losses.

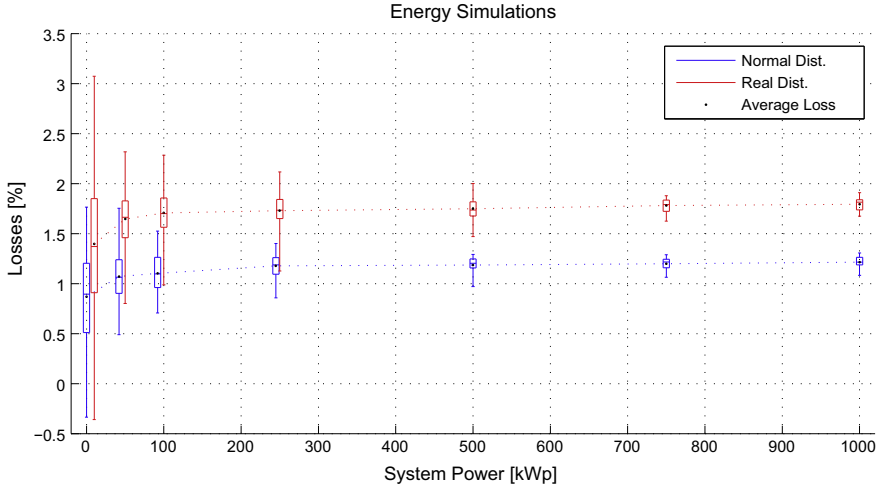

Fig. 3. Energy losses.

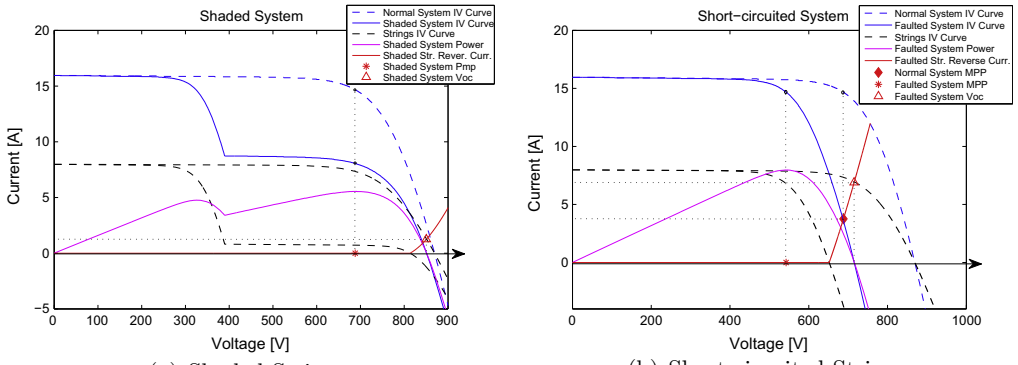

(a) Shaded String. (b) Short-circuited String.

Fig. 4. Reverse current in a shaded and short-circuited string.

and a fusing current $I_f = 1.45 \cdot I_n$, it also specifies a conventional time for PV fuse-links that for $I_n \leqslant 63$ amperes is equal to 1 h. For a short-circuit case, it is necessary that the inverter takes longer than one hour to find the new MPP to damage the fuse and thus is not very likely.

With large system powers, the influence of a shaded or short-circuited string over MPP and Voc of the system may be different, so the simulations were repeated with different system sizes, using modules without parameter variations (all the modules were set with datasheet

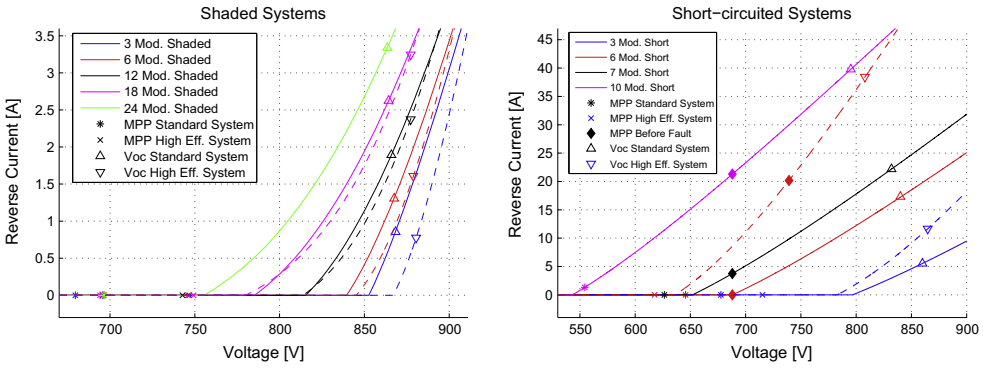

(a) Standard & High Efficiency Shaded Strings.

(b) Standard & High Efficiency Short-circuited Strings.

Fig. 5. Reverse current in a shaded and short-circuited string.

parameters) so the same system was used in each simulations.

Firstly, the size of the system was increased by adding more strings (and therefore current), keeping the voltage (modules per strings) constant. For the shaded scenario, all the modules of the string were fully shaded (a 90% irradiance reduction) for both systems (standard silicon and high efficiency). For the short-circuited scenario a short-circuit sufficient to cause a reverse current twice the Isc of the modules was introduced. For the standard silicon system 10 of 24 modules were short-circuited in 1 string, and for the high efficiency system 6 of 18 modules. Fig. 6 shows the results of these simulations.

As shown in Fig. 6(a), there is almost no difference in the reverse current in the shaded string when the size (power) of the system was increased. When the size of the system was increased by 1000%, the reverse current increased by 6.8% in the standard silicon system and by 8.4% in the high efficiency system.

As shown in Fig. 6(b), for the short-circuited case, when the system size was increased by 400%, the reverse current at the final MPP (∗) was twice the Isc in the standard silicon system and almost twice Isc in the high efficiency system. This final reverse current is sufficient to break the DC fuse of the string. If the inverter switches off in this scenario or starts re-tracking the MPP from Voc for any reason, the reverse current could reach 5–6 times the STC Isc.

After increasing the system current, the voltage of the system was increased adding more modules per string in a 50 string system. For the shaded scenario all the modules of the string were fully shaded (90% irradiance loss) for both systems (standard silicon and high efficiency). For the short-circuited scenario a number of modules were short-circuited to obtain a reverse current of twice the module Isc. Fig. 7 shows the results of these simulations.

As can be seen in Fig. 7(a), there is almost no difference in the reverse current in the shaded string when the voltage of the system was increased, this is because to increase the voltage of the system, more modules per string would have to be added, increasing also the resistance of the string (there is a linear relationship between the increase of voltage and resistance).

As shown in Fig. 7(b), for a system Voc around 800 [VDC], its necessary for 10 of 24 modules to be short-circuited (42% of the string) to have a reverse current over two times Isc in the standard silicon system and 6 of 18

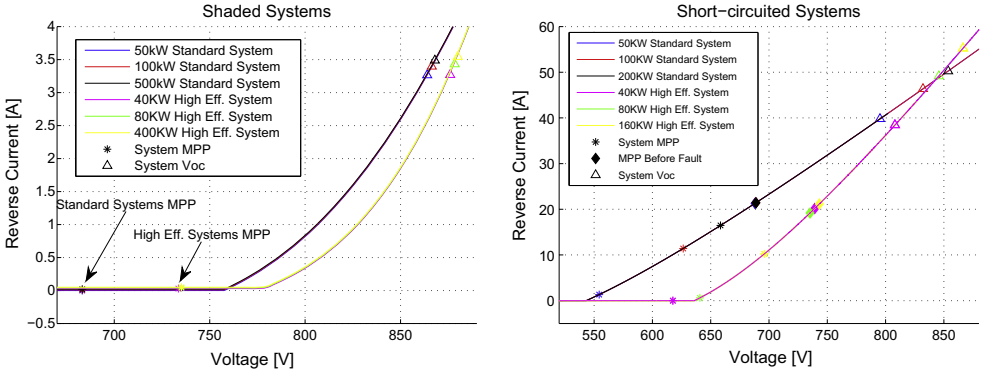

(a) Standard Silicon & High Efficiency Shaded Strings.

(b) Standard Silicon & High Efficiency Short-circuited Strings.

Fig. 6. Reverse current in shaded & short-circuited String With Different Systems Size.

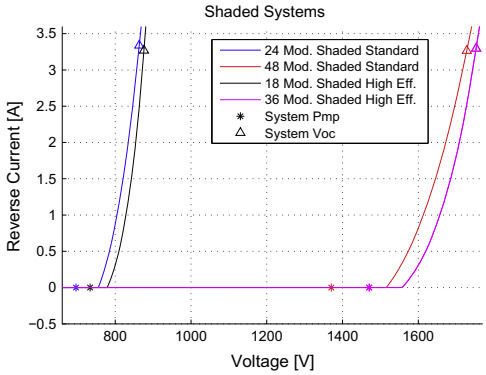

(a) Standard Silicon & High Efficiency Shaded Strings.

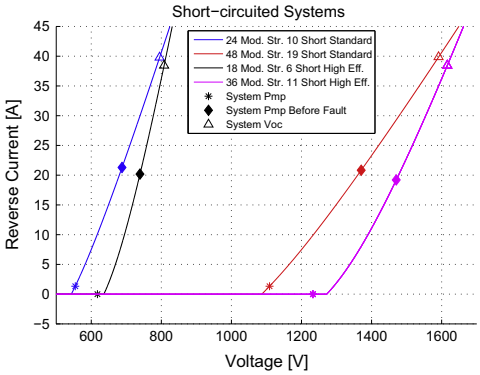

(b) Standard Silicon & High Efficiency Short-circuited Strings.

Fig. 7. Reverse Current in a shaded & short-circuited string with different voltages.

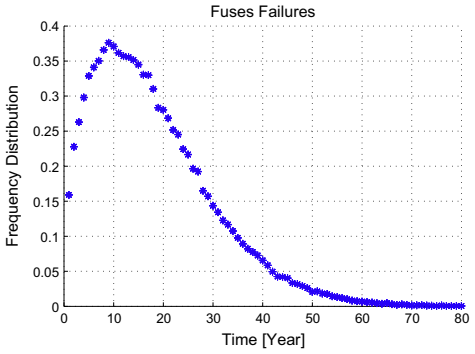

(a) Fuses Failures Frequency Distribution.

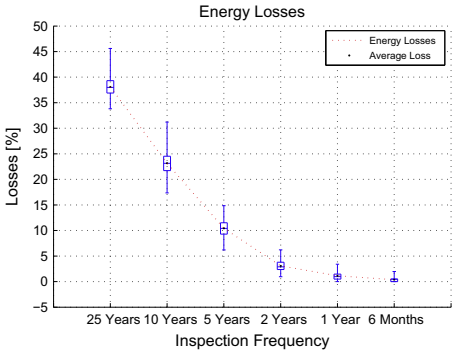

(b) Energy Losses due to Fuses Failures.

Fig. 8. Fuses failures.

(33% of the string) in the high efficiency system. For a system Voc around 1600 [VDC], are necessary 19 of 48 short-circuited modules (40% of the string) in the standard silicon system and 11 of 36 (31% of the string) in the high efficiency system.

3.5. Fuses failures and their impact on system performance

String fuses have the possibility to fail due to other failures in the system depending on the mean time to failure (MTTF) of individual components. To estimate the energy losses due to these fuse failures, the MTTF feature was added to the string fuses of the model and then 100 simulations were performed using a 1 MWp system, considering a system lifetime of 25 years. In each simulation new fuses were generated with its respective MTTF. Different inspection periods were performed, where the failed fuses were replaced, generating new fuses with a new MTTF. Fig. 8(a) shows the frequency distribution of the MTTF of the fuses generated in the simulations. Fig. 8(b) shows the energy losses when different inspection periods were performed.

As shown in Fig. 8(b) the energy losses due to fuse failures without inspections reach 38%. With an annual inspection the losses are reduced to a 1% and with an inspection every 6 months the losses are reduced to a 0.6%.

4. Conclusion

PV systems over 3.6 MWp with modules power tolerance of ±3%, start to present mismatch energy losses over 2%. The loss of energy is more significant than the loss of rated power in the system. The latter is closer to half the power tolerance. This is just for the system alone and does not include any other effects such as slight differences in orientation that will further enhance this effect. As the majority of system specifications is based on positive power, this means that any gains achievable with this power will be more than negated by any additional orientation. It also means, however, that one could enhance the yield 0.5% by pre-sorting modules for systems smaller than 100kWp, but for larger systems the benefits reduce quickly.

It appears that the use of thermal fuses for overcurrent protection has been carried over from their traditional use

in circuits supplied by batteries or electromagnetic generators to the DC circuits of PV systems without modification for the specific failure modes in PV systems. Based on the results presented here, it is not clear that thermal fuses provide the intended protection.

There is no relevant reverse current due to partial or full shading of strings in a PV system with fully operational bypass diodes and inverter(s). In extreme shading scenarios, where a whole string was shaded by 90%, the reverse current was less than the short circuit current of the modules.

The use of string fuses does not ensure fault clearance due to the action of the inverter. Fault reverse currents are determined by fault types, fault location and the action of the MPP tracking algorithm of the inverter. There are some faults that are hidden by the inverter action, because when the failure occurs, the inverter negates the fault reverse current by reducing the voltage of the system, before the fuses disconnection time is reached. If the inverter is disconnected however, the fault reverse current can be 5 times the short circuit current of the modules. Thus, it one would need two faults in the system to cause a reverse current fault of a magnitude that would destroy the modules. In these cases, it is questionable if a one h withstand time of the fuses delivers the required protection.

The use of string fuses does not prevent the risk of reverse currents. In shaded scenarios, the reverse current in the strings was lower than the fusing current. In short-circuited scenarios, in most cases the inverter reduced the fault reverse current to levels below the fuse disconnection current. In both cases (shading and short-circuits), the reverse currents involve significant losses that justify the use of series blocking diodes in the strings. The question of the economically most beneficial approach would then need to be answered based on the reliability of all the components involved.

A study of 180 fires involving PV systems found that in 50% of cases the fires were caused by installer errors not by component failures (TVRheinland, 2012). The use of DC string fuses adds complexity to systems and may increase the number of DC connections to be made on site by installers. As such the uses of thermal fuses could increase the risk of fires in PV systems.

The PV industry should review the protection strategy for PV systems and consider whether the current combination of module bypass diodes and string fuses is the best solution.

Assuming 1–2 string fuses failures per system lifetime, as reported in the literature, with a failure rate that increase with time, the energy losses without an inspection and replacement plan are very significant (38%). These losses can be almost eliminated with an annual inspection plan. The current approach of string monitoring will show any failures quickly and will guarantee minimal losses due to failures. A detailed of the energy losses versus protection of the system is yet outstanding.

Acknowledgment

This work has been supported in parts by a joint UK-India initiative in solar energy through a joint project 'Stability and Performance of Photovoltaics (STAPP)' funded by Research Councils UK (RCUK) Energy Programme in UK (contract no: EP/H040331/1) and by Department of Science and Technology (DST) in India. The funders were not directly involved in the content of this article. Underlying research data may be available from the corresponding author.

Appendix A. PV modules parameters distributions

See Figs. A.9–A.11.

Appendix B. Power and energy simulations

See Tables B.2 and B.3.

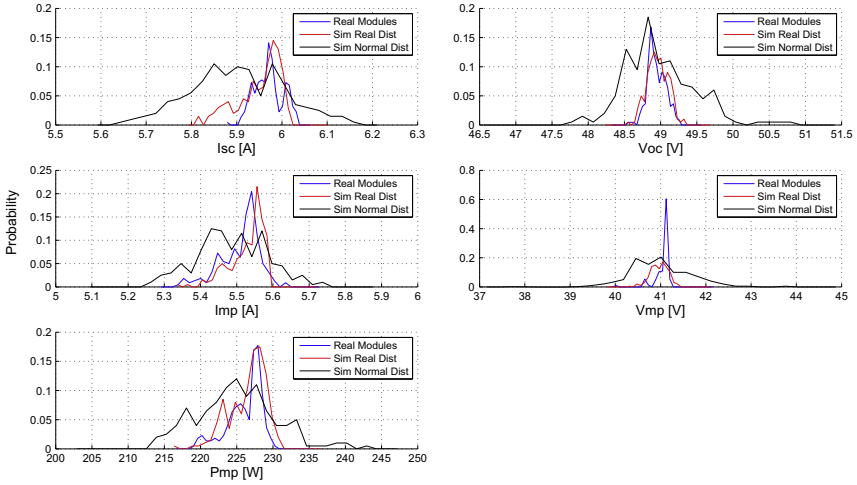

Fig. A.9. High efficiency modules parameters distributions.

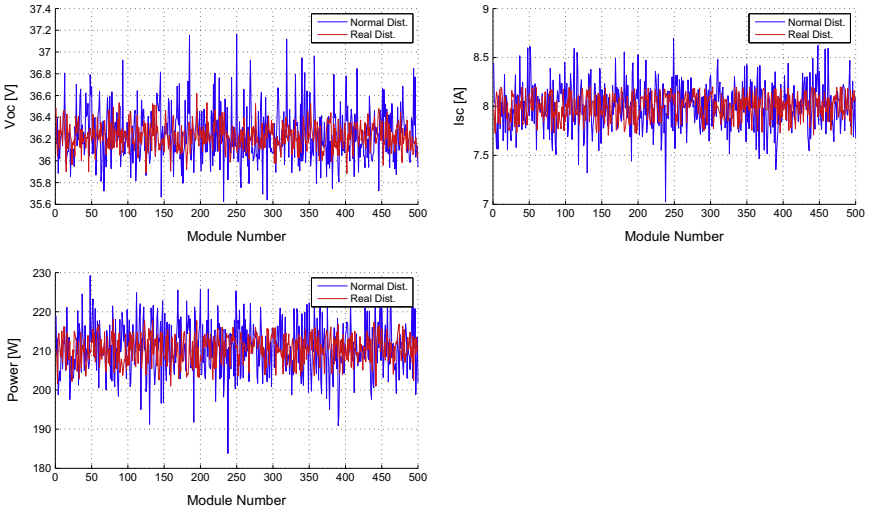

Fig. A.10. Standard silicon modules distribution.

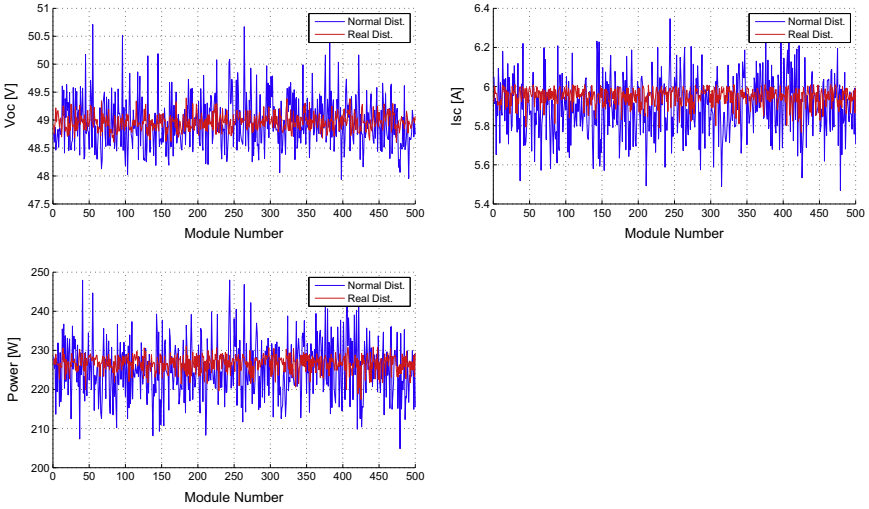

Fig. A.11. High efficiency modules distribution.

Table B.2
Power simulations with different distributions.

Power simulations							
	Normal distribution						
Number of simulations	100	100	100	100	100	100	100
Power without variance [kWp]	10.11	50.53	101.05	252.63	505.27	757.90	1010.53
Average power with variance [kWp]	10.04	50.20	100.35	250.79	501.64	752.41	1003.24
Average loss [%]	0.64	0.65	0.70	0.73	0.73	0.73	0.72
Power std. dev. [%]	0.53	0.24	0.16	0.10	0.07	0.06	0.06
Max. power [kWp]	10.20	50.47	100.69	251.33	502.45	753.79	1004.47
Min. power [kWp]	9.91	49.89	99.94	250.18	500.82	751.19	1001.18
	Real distribution						
Number of simulations	100	100	100	100	100	100	100
Power without variance [kWp]	10.11	50.53	101.05	252.63	505.27	757.90	1010.53
Average power with variance [kWp]	9.98	49.86	99.73	249.26	298.54	747.72	997.03
Average loss [%]	1.21	1.32	1.31	1.33	1.33	1.34	1.34
Power std. dev. [%]	0.74	0.33	0.23	0.14	0.13	0.08	0.06
Max. power [kWp]	10.13	50.23	100.40	250.26	500.13	749.21	998.64
Min. power [kWp]	9.76	49.51	99.05	248.39	497.12	746.00	995.14

Table B.3
Energy simulations with different distributions.

Energy simulations							
	Normal distribution						
Number of simulations	100	100	100	100	86	36	10
System power [kWp]	10	50	100	250	500	750	1000
Energy without variance [MWh]	8.95	44.75	89.49	223.73	447.46	671.19	894.92
Average energy with variance [MWh]	8.87	44.27	88.50	221.10	442.16	663.15	884.05
Average loss [%]	0.87	1.07	1.10	1.18	1.19	1.20	1.21
Energy std. dev. [%]	0.49	0.23	0.19	0.12	0.08	0.07	0.07
Max. energy [MWh]	8.98	44.53	88.86	221.81	443.12	664.05	885.23
Min. energy [MWh]	8.79	43.96	88.13	220.59	441.68	662.55	883.24
	Real distribution						
Number of simulations	100	100	100	100	74	48	42
System power [kWp]	10	50	100	250	500	750	1000
Energy without variance [MWh]	8.95	44.75	89.49	223.73	447.46	671.19	894.92
Average energy with variance [MWh]	8.82	44.01	87.96	219.86	439.64	659.25	878.88
Average loss [%]	1.40	1.65	1.71	1.73	1.75	1.78	1.79
Energy std. dev. [%]	0.67	0.32	0.24	0.16	0.11	0.07	0.06
Max. energy [MWh]	8.98	44.39	88.61	221.21	440.89	660.29	879.94
Min. energy [MWh]	8.67	43.71	87.45	219.00	438.51	658.58	877.84

References

Bishop, J.W., 1988. Computer simulation of the effects of electrical mismatches in photovoltaic interconnection circuits. Sol. Cells, 73–89.

Calais, M., Wilmot, N., Ruscoe, A., Arteaga, O., Sharma, H. 2008. Over-current protection in PV array installations. In: ISES-AP – 3rd International Solar Energy Society Conference – Asia Pacific Region (ISES-AP-08) Incorporating the 46th ANZSES Conference, pp. 1–12.

Gomez, D., Pedrazzi, S., Zini, G., Dalla Rosa, A., Tartarinib, P., 2014. Mismatch losses in PV power plants. Sol. Energy 100, 42–49.

Goss, B., Reading, C., Gottschalg, R., 2011. A review of overcurrent protection methods for solar photovoltaic DC circuits. In: 7th Photovoltaic Science, Applications and Technology Conference (PVSAT-7), pp. 1–5.

Goss, B., Cole, I.R., Betts, T.R., Gottschalg, R., 2014. Irradiance modelling for individual cells of shaded solar photovoltaic arrays. Sol. Energy 110, 410–419.

Herrmann, W., 2005. Analyses of array losses caused by electrical mismatch of PV modules. In: 20th European Photovoltaic Solar Energy Conference, pp. 1–4.

IEC-60269, 2010. Low-voltage fuses – Part 6: supplementary requirements for fuse-links for the protection of solar photovoltaic energy systems. In: IEC (International Electrotechnical Commission).

IEC-60364, 2005. Low-voltage electrical installations. In: IEC (International Electrotechnical Commission).

IEC-62109, 2010. Safety of power converters for use in photovoltaic power systems. In: IEC (International Electrotechnical Commission).

Johansson, A., Gottschalg, R., Infield, D.G., 2004. Effect of shading on amorphous silicon single and double junction photovoltaic modules. Int. J. Ambient Energy 25, 65–72.

Laschinsky, J., Bettenwort, G., Herbst, L., Merz, C., Zanger, S., 2010. Reverse currents of PV modules origin and prediction. In: 25th European Photovoltaic Solar Energy Conference and Exhibition/5th World Conference on Photovoltaic Energy Conversion, pp. 1–3..

MacAlpine, S., Brandemuehl, M., Erickson, R., 2012. Beyond the Module Model and into the Array: Mismatch in Series. University of Colorado, pp. 1–5.

Mohapatra, P., 2011. Simulation of Partial-shading Effects on PV Arrays via Diode Modeling. Loughborough University, pp. 1–14.

Perdue, M.R., Gottschalg, R., 2015. Energy yields of small grid connected PV systems: Effects of Component Reliability and Maintenance. IET Renew. Power Gen., in press.

Quaschning, V., Hanitsch, R., 1996. Numerical simulation of current–voltage characteristics of photovoltaic systems with shaded solar cells. Sol. Energy 56 (6), 513–520.

TVRheinland, 2012. German research project: fire safety risks at PV systems and risk minimization. In: Photon Workshop 4. PV SAFETY.